# Chemical Kinetic Modeling of High Pressure Propane Oxidation and Comparison to Experimental Results

**David N. Koert**
Mechanical Engineering Dept., Wichita State University, Wichita, KS 67260

**William J. Pitz**
Lawrence Livermore National Laboratories, Livermore, CA 94551

**Joseph W. Bozzelli**
Chemistry and Chemical Engineering Department, New Jersey Institute of Technology,
Newark, NJ 07102

**Nicholas P. Cernansky**
Depart. of Mechanical Engineering and Mechanics
Drexel University, Philadelphia, PA 19104

May 6, 1996

Accepted for Presentation at Twenty-Six International Symposium on Combustion
Universita Federico II, Napoli, Italy
28 July -2 August 1993

Oral Presentation
Colloquium topic area: General Reaction Kinetics
Word count:
5482 total words = 2682 text + 2 figs @ 800 words + 2 figs @ 400 +
2 tables @ 200 words

Corresponding author:
William J. Pitz, L-14
Lawrence Livermore National Laboratory
Livermore, CA 94551
phone: (510) 422-7730
fax: (510) 422-2644
email: pitz@llnl.gov

# Chemical Kinetic Modeling of High Pressure Propane Oxidation and Comparison to Experimental Results

**David N. Koert**
Mechanical Engineering Dept., Wichita State University, Wichita, KS 67260

**William J. Pitz**
Lawrence Livermore National Laboratories, Livermore, CA 94551

**Joseph W. Bozzelli**
Chemistry and Chemical Engr. Depart., New Jersey Inst. of Tech., Newark, NJ 07102

**Nicholas P. Cernansky**
Depart. of Mechanical Engineering and Mechanics
Drexel University, Philadelphia, PA 19104

## ABSTRACT

A pressure dependent kinetic mechanism for propane oxidation is developed and compared to experimental data from a high pressure flow reactor. Experimental conditions range from 10-15 atm, 650-800 K, and a residence time of 198 ms for propane-air mixtures at an equivalence ratio of 0.4. The experimental results clearly indicate a negative temperature coefficient (NTC) behavior. The chemistry describing this phenomena is critical in understanding automotive engine knock and cool flame oscillations. Results of the numerical model are compared to a spectrum of stable species profiles sampled from the flow reactor.

Rate constants and product channels for the reaction of propyl radicals, hydroperoxy-propyl radicals and important isomers (radicals) with $O_2$ were estimated using thermodynamic properties, with multifrequency quantum Kassel Theory for k(E) coupled with modified strong collision analysis for fall-off.

Results of the chemical kinetic model show an NTC region over nearly the same temperature regime as observed in the experiments. Sensitivity analysis identified the key reaction steps that control the rate of oxidation in the NTC region. The model reasonably simulates the profiles for many of the major and minor species observed in the experiments.

Numerical simulations show some of the key reactions involving propylperoxy radicals are in partial equilibrium in this residence-time, temperature and pressure regime. This indicates that their relative concentrations are controlled by a combination of thermochemistry and other rate-controlling reaction steps. Major reactions in partial equilibrium include $C_3H_7 + O_2 = C_3H_7O_2$, $C_3H_6OOH = C_3H_6 + HO_2$ and $C_3H_6OOH + O_2 = O_2C_3H_6OOH$. This behavior means that thermodynamic parameters of the oxygenated species, which govern partial equilibrium concentrations, are especially important. QRRK/fall-off results also show that the reaction of propyl radical and hydroperoxy-propyl radicals with $O_2$ proceeds, primarily, through pressure-stabilized adducts, not chemically activated channels; thus dissociation and isomerization rates of these adducts are important.

## INTRODUCTION

The combustion of hydrocarbons in practical combustion devices such as internal combustion (I.C.) engines and gas turbines occurs at pressures well above atmospheric conditions where most experimental flame and thermal reaction studies are conducted. The development and validation of chemical kinetic mechanisms at elevated pressures are needed to obtain accurate models of fuel oxidation rates in these combustion devices. Reaction mechanisms validated at these high pressures can then be applied to understand and to predict improvements in problems such as engine knock and hydrocarbon emissions. In this study, a pressure-dependent kinetic mechanism for propane oxidation is developed and compared to experimental data from a high pressure flow reactor.

Experimental data from a pressured flow reactor (PFR) were used to validate the chemical kinetic mechanism. The PFR apparatus [1] complements other experimental apparatus (rapid compression machine, motored and fired I.C. engine) for the study of hydrocarbon oxidation related to automotive engine knock. A key advantage of the PRF is that the temperature, pressure and residence time of the fuel-air mixture are all well-characterized and controlled. The temperature history of the reacting gases is maintained at a nearly constant, measured value. The effect of wall interactions on the gas-phase chemistry are also minimized in the PFR.

There is a significant amount of data in the literature on propane oxidation, but few investigations have reported data in a pressured flow reactor over the NTC region. One of the unique features of the PFR data [2] used in this study, is that it exhibits a clear and dramatic NTC region from 720-780 K that was not reported in other flow and stirred reactor studies [3-5]. These previous studies investigated propane oxidation at higher pressures, but focused on temperatures that exceeded the regime where NTC behavior is observed. NTC behavior has been observed in lower pressure studies of propane oxidation in static reactors [6]. In the following sections of the paper, the development of the chemical kinetic model is described and the experimental technique is documented. The results of the chemical kinetic model are compared to the experimental results. Finally, key findings from the kinetic modeling study are discussed.

## CHEMICAL KINETIC MODEL

The chemical kinetic mechanism was based on previous studies [7], with substantial improvements being made. As will be shown later, many of the important reactions involving alkylperoxy and related species are in partial equilibrium, so that it is essential to address properly the thermodynamic properties (enthalpy and entropy) of the species that control the equilibrium. Thermodynamic properties listed in Table 1 for the relevant radicals and stable parents were obtained by group additivity using THERM [8] with updated H/C/O groups and bond dissociation groups [9]. Abinitio calculations and isodesmic reaction analysis were performed for selected peroxides [10]. The thermochemical data allow accurate calculation of reverse reaction rate constants by microscopic reversibility.

The rate of decomposition of hydrogen peroxide is critical in controlling the location of the end to the NTC region, as discussed later. We use the recent rate-constant expression of Marinov and Malte [11] which gives a nine parameter, pressure dependent fit. Use of this reaction rate expression improved the agreement between the measured and calculated propane consumption at the end of the NTC region.

The propyl peroxy and hydroperoxy-propyl [12] isomerizations are important reactions controlling the chemistry of the NTC region. The activation energy ($E_a$) for the forward rate of these reactions is estimated by,

$$E_a = \text{ring strain} + E_{abst}\begin{matrix}\text{primary}\\ \text{secondary}\\ \text{tertiary}\end{matrix} + \Delta U_{rxn}$$

where $\Delta U_{rxn}$ is the potential energy change for the reaction (only included if reaction is endothermic). The ring strains are 6.0, 0.1, and 6.0 kcal/mole for heterocyclic rings (including peroxy moiety) containing five, six, and seven members respectively [13]. The ring strains were validated with comparisons of modeling and experimental results on the ethyl + $O_2$ reaction system [14] and by ab initio calculations. The activation energy for abstraction ($E_{abst}$) was estimated from the reverse reaction (exothermic direction). The reverse reaction is assumed to have

an $E_{abst}$ which is the same as an alkyl radical abstracting an H-atom from a propylhydroperoxide,

$$CCCOOH + R. = CCCOO. + RH$$

where R is an alkyl radical and carbon atoms are assumed to be fully saturated with H atoms. The activation energy of this reaction was estimated from an Evans-Polanyi plot ($E_{abst}$ versus $\Delta H_{rxn}$) [15] of the similar H-atom abstraction reaction, RH + R.' = R. + R'H. A reduction of 0.3 kcal/mole in $E_{abst}$ for each kcal/mole reduction in $\Delta H_{rxn}$ was obtained.

Pre-exponential factors for the $RO_2$ isomerization were obtained using RADICALC [16], a computer code which implements transition state theory. The pre-exponential factors were validated from detailed model comparisons to experimental results on ethyl, tert-butyl, iso-butenyl and neo-pentyl radical reactions with $O_2$. Results of the calculations show that the loss of internal rotors is the major contribution to the loss of entropy and thus reduction in Arrhenius pre-exponential factor with increasing ring size in the transition state. The rate constants of $RO_2$ isomerization are given in Table 2.

Rate constants and product channels for the reaction of propyl and hydroperoxy-propyl radicals with $O_2$ and the reaction of important adducts were estimated with multifrequency quantum Kassel Theory (QRRK) [17,18] for k(E) coupled with modified strong collision analysis for fall-off. QRRK approximations and their implications for rate constant estimation are given in Reference 17.

The numerical model assumed constant temperature and pressure, and plug flow, in the flow reactor experiments.

## EXPERIMENTAL TECHNIQUE

The Pressured Flow Reactor (PRF) has been described previously [2] and is only summarized here. A 2.5 cm diameter Vycor reactor is housed in a stainless steel pressure vessel. Reactant gases are metered with mass flow controllers. The experiments covered a range from 650-850 K and pressures of 10 and 15 atm for a residence time of 198 ± 2 ms. Propane/air mixtures were maintained at an equivalence ratio of 0.4. The initial concentration of propane and oxygen was the

same in each experiment (2.47 $mol/m^3$ at 800K), with the balance of the flow consisting entirely of nitrogen.

Samples of the reacting gases were withdrawn with a glass-lined, water-cooled gas sampling probe. Samples were extracted at constant residence time (198 ms) at different reactor temperatures by adjusting the axial position of the sampling probe during the experiment. Samples were analyzed on a Varian 3740 gas chromatograph (GC) with a Porapak Q column followed by a Porapak N column and a flame ionization detector (FID). A postcolumn heated catalyst consisting of powder nickel was used to methanize the oxides of carbon to increase the sensitivity of their measurement by FID.

## RESULTS

The results of the numerical model are compared to the experimentally measured results in Figs. 1-3. The species profiles at 10 atm looked similar to those at 15 atm. Figure 1 shows the propane consumption across the NTC region at 10 and 15 atm. Both the model and experiments show a distinct NTC region. The characteristic shape of the profiles is well reproduced by the model.

Intermediate species profiles are shown in Figs. 2 and 3. The measured and calculated carbon monoxide profiles agree reasonably well. The calculated peak of the propene profile in excellent agreement at 10 atm (Fig. 2) and 15 atm (Fig. 3). The main reactions producing propene are discussed below. The predicted maximum concentration of formaldehyde is 3.5 and 15 times high at 10 and 15 atm respectively compared to the measured values. The measured formaldehyde may be under-reported because of polymerization to paraformaldehyde in the G.C. column. This explains some but not all of the discrepancy between the calculation and measurement. The acetaldehyde peak concentration is a factor of 3 high at 10 atm and 15 atm compared to the measured concentration. The calculated ethylene concentration is low compared to the measured by about a factor of 3. The calculated carbon dioxide concentrations are below the measured by a factor of 2-3.

A number of minor species were measured and compared to calculated values. Methanol is predicted to be a factor of 5 higher than observed in the experiments. The calculated maximum concentration of acrolein is about 20 times higher than the

measured maximum. The peak concentration of propene oxide is a factor of 2 low at 10 atm and factor of 4 low at 15 atm. Propene oxide, a key indicator of propylperoxy isomerization, is produced from the decomposition of the hydroperoxy-propyl radicals whose decomposition rate constant was calculated using QRRK. This reaction is identified as being important in the sensitivity analysis discussed below. The calculated propionaldehyde concentrations compare very well with the experimental values. The predicted acetone concentrations (not shown) were an order of magnitude below the experimental values.

Sensitivity analysis was performed by multiplying the rate constant of an individual reaction by a factor of two, computing the final propane concentration at 735 K and 790 K, and calculating the percent change compared to the baseline case. A positive percent change indicates a decreased overall reaction rate and a negative percent changes indicates an increased overall reaction rate. The temperatures 735 K and 790 K represent onset and end of the NTC region at 15 atm, respectively (Fig. 1). The reaction rate constants that exhibited the highest sensitivity are shown in Fig. 4. The reaction with the top sensitivity is the production of propene from hydroperoxy-propyl:

$$C.{}_3H_6OOH \leftrightarrow C_3H_6 + HO_2 \qquad (1)$$

This reaction has the largest inhibiting effect on the overall oxidation rate and plays a major role producing NTC behavior as previously described in the literature [20].

The reaction exhibiting the second highest sensitivity is H-atom abstraction from the fuel by OH radicals. The rate of this reaction is well-known and taken from Droege and Tully [19]. Hydrogen peroxide decomposition gives the third highest sensitivity. This reaction is important in controlling the overall reaction rate at the end of the NTC region (790 K) and has comparatively little effect at the onset of NTC. The high sensitivity shown by

$$O_2C_3H_6OOH \rightarrow HOOR'CHO + OH$$

indicates the important role of the addition of $O_2$ to hydroperoxy-propyl giving $O_2C_3H_6OOH$ and leading to subsequent OH production and branching. The pressure and temperature dependence of the decomposition rate constant of above reaction was calculated by QRRK.

Analysis of the reaction paths described by the numerical simulations show many interesting features. Several key reactions are in partial equilibrium so that the relative concentrations of species are controlled by thermochemistry. These major reactions include the addition of propyl and hydroperoxy-propyl to $O_2$:

$$C_3H_7 + O_2 \leftrightarrow C_3H_7O_2$$
$$C.{}_3H_6OOH + O_2 \leftrightarrow O_2C_3H_6OOH \quad .$$

Careful estimation of thermodynamic parameters for the species in these reactions was important to achieve the proper partial equilibrium. Additionally, reverse rates controlled by thermochemical parameters were important for Reaction 1 that produces propene. Reverse rates computed from thermochemistry were 10-15% of the forward rates.

One key issue addressed in this study are chemically-activated reactions involving the addition of propyl and hydroperoxy-propyl radicals to molecular oxygen. In the case of propyl radicals, a fraction of the chemically excited adducts formed from the addition reacts to propene and $HO_2$:

$$C_3H_7 + O_2 \rightarrow C_3H_6 + HO_2 \qquad (2).$$

The most rapid rate was found at the end of the NTC region (770-780 K) where ca. 10% of the propene is produced by the chemically activated path. The remaining propene (ca. 90%) is produced through stabilized adducts (Reaction 1). In the case of hydroperoxy-propyl addition to molecular oxygen, the chemically-activated paths contribute less than 0.5% of the overall addition process. Almost all the molecular addition proceeds through stabilized adducts:

$$C.{}_3H_6OOH + O_2 \leftrightarrow O_2C_3H_6OOH \rightarrow \text{products}$$

The present study indicates the importance of a new path for the consumption of the adduct $O_2C_3H_6OOH$. The adduct can react by two paths, the first of which (Reaction 3) is frequently mentioned in the literature [20]:

$$.OOCCCOOH \rightarrow HOOCCC{=}O + OH \qquad (3)$$
$$\rightarrow HOOCC.COOH \rightarrow C{=}CCOOH + HO_2 \qquad (4)$$

(The carbon atoms are assumed to be fully saturated with H atoms, the dot indicates a radical site on the left, adjacent carbon atom. The above example shows the consumption of one of the three possible $O_2C_3H_6OOH$ isomers). The second path (Reaction 4) involves abstraction of the H atom from the non-oxygenated carbon by

the peroxy moiety and has been noted recently [12]. Calculations show that the second path accounts for 5-30% of the consumption (by isomerization) of the $O_2C_3H_6OOH$ adducts at the start of the NTC region, with the remaining 70-90% consumed by Reaction 3. Reaction 3 accelerates the oxidation process (as seen in Fig. 4) because it produces a reactive OH radical while Reaction 4 produces a relatively unreactive $HO_2$ radical. This analysis indicates it may be important to include the newly-considered path (Reaction 4) to achieve the proper overall rate for propane oxidation.

## CONCLUSIONS

Many features of high pressure flow reactor experiments illustrating the NTC regime are reasonably simulated with a newly developed mechanism for propane oxidation. Further work will be needed to resolve differences between predicted and measure aldehyde levels. In the mechanism development, the thermodynamic parameters of the peroxy and hydroperoxy $C_3$ species were carefully estimated. These properties control the partial equilibrium of key reactions involving the addition of propyl and hydroperoxy-propyl to molecular oxygen. Chemically-activated reaction paths associated with these additions were also estimated by QRRK/fall-off analysis. In the case of propyl addition to $O_2$, the chemically activated reaction paths contributed about 10% of the propene production at the end of the NTC region, with the majority of propene production occurring through stabilized adducts. In the case of hydroperoxy-propyl addition to $O_2$, the chemically activated paths contributed less than 0.5%, with almost all the addition proceeding through stabilized adducts. These results indicate that for propane oxidation at 10 and 15 atm across the NTC region, these chemically activated paths make a minor contribution.

## ACKNOWLEDGMENTS

The authors greatly appreciate valuable discussions with Dr. Henry Curran, Dr. Nick Marinov and Dr. Charles Westbrook of Lawrence Livermore National Laboratory. The experimental work at Drexel University was carried out under ARO contract No. DAAH04-93-G-0042 and NSF grant no. CTS 9213501. The portion

of this work at Wichita State University was funded by the National Institute for Aviation Research. The work at LLNL was carried out under the auspices of the U. S. Department of Energy by the Lawrence Livermore National Laboratory under contract No. W-7405-ENG-48.

## REFERENCES


1. Koert, D.N. and Cernansky, N.P., *Meas. Sci. Technol. (formerly J. Phys. E)* 3:607-613, 1992.
2. Koert, D.N., Miller, D.L. and Cernansky, N.P. *Combust. Flame* 96:34-49 (1994).
3. Dagaut, P., Cathonnet, M., Boettner, J.C., and Gaillard, F. *Combust. Sci. and Tech.* 56:23-63 (1987).
4. Hoffman, J.S., Lee, W., Litzinger, T. A., Santavicca, D. A., and Pitz, W. J., *Combust. Sci. Technol.* 77:95 (1991).
5. Cathonnet, M., Boettner, J.C., and James, H., Eighteenth Symposium (International) Combustion, The Combustion Institute, Pittsburgh, 1981, p. 903.
6. Wilk, R. D., Cernansky, N. P., and Cohen, R. S. *Combust. Sci. and Tech.*, 49:41-78 (1986).
7. Pitz, W. J., Westbrook, C. K., and Leppard, W. R., "Autoignition Chemistry of $C_4$ Olefins Under Motored Engine Conditions: A Comparison of Experimental and Modeling Results," *SAE Transactions*, SAE paper SAE-912315 (1991).
8. Ritter, E. R. and Bozzelli, J. W. *Int. J. Chem. Kinet.* 23:767(1991).
9. Lay, T., Bozzelli, J. W., Dean, A. M., and Ritter, E. R. *J. Phys. Chem.* 99:14514 (1995).
10. Lay, T., Krasnoperov, L., Venanzi, C., and Bozzelli, J. *J. Phys. Chem.*, 100:xx (1996).
11. Nick Marinov, N. M. and Malte, P. C. *Int. J. Chem. Kin.* 27:957 (1995).
12. Bozzelli, J.W. and Pitz, W.J. Twenty-Fifth International Symposium on Combustion, The Combustion Institute, Pittsburgh, PA, 1994, p. 783-791.
13. Dorofeeva, O. V., Gurvich, L. V., and Jorish, V. S. *J. Phys. Chem. Ref. Data* 15:437-464 (1986).
14. Bozzelli, J.W., and Dean, A.M. *J. Phys. Chem*. 94:3313 (1990).
15. Evans, M. G. and Polanyi, M. *Trans. Faraday Soc.* 34:11 (1938).

16. Ritter, E. R., and Bozzelli, J. W., *Chemical and Physical Processes in Combustion,* The Combustion Institute, Pittsburgh, PA, 1993, #103, p. 459.

17. Dean, A. M., *J. Phys. Chem.* 89:4600 (1985).

18. Dean, A. M., Bozzelli, J. W., Ritter, J. W. *Combust. Sci. Tech.* 80:63-85 (1991).

19. Droege, A.T. and Tully, F.P., *J. Phys. Chem.* 90:1949 (1986).

20. Benson, S. W. *Prog. Energy Combust. Sci.* 7:125-134 (1981).

## FIGURE CAPTIONS

Figure 1. Comparison of the experimental and calculated fuel consumed: A. 10 atm. B. 15 atm

Figure 2. Comparison of the experimental and calculated species concentrations at 10 atm. (Experimental results are on the left and calculated results on the right).

Figure 3. Comparison of the experimental and calculated species concentrations at 15 atm. . (Experimental results are on the left and calculated results on the right).

Figure 4. Sensitivity results at 15 atm. (RH is propane; R is propyl; RO2 is $CH_3O_2$, $C_2H_5O_2$ and $C_3H_7O_2$; XO2 is $HO_2$ and $CH_3O_2$; c-C3H6O is a $C_3$ cyclic ether; and HOOR'CHO is a $C_3$ ketohydroperoxide.)

Table 1: Thermochemical Properties of Important Species

| Species | $\Delta H^{\circ}_{f\ 298}$ | $S_{298}$ |
|---|---|---|
| $HO_2$ | 3.80 | 54.73 |
| $CH_3OO.$ | 4.50 | 65.84 |
| $C.H_2OOH$ | 14.80 | 67.53 |
| $CH_3OOH$ | -31.60 | 65.62 |
| CCOO. | -4.99 | 75.75 |
| C.COOH | 7.91 | 78.94 |
| CC.OOH | 2.81 | 79.35 |
| .OOCCOOH | -25.68 | 94.82 |
| HOOC.COOH | -17.88 | 98.42 |
| CCOOH | -41.09 | 75.53 |
| HOOCCOOH | -61.78 | 94.60 |
| C.CCOOH | 2.98 | 89.74 |
| CC.COOH | 0.33 | 89.39 |
| CCC.OOH | -2.12 | 88.77 |
| CCCOO. | -9.92 | 85.17 |
| $C_2COO.$ | -12.48 | 82.30 |
| $C_2.COOH$ | 0.42 | 86.88 |
| $C_2C.OOH$ | -7.08 | 88.06 |
| HOOC.CCOOH | -30.61 | 104.24 |
| HOOCC.COOH | -20.36 | 108.46 |
| HOOC.CCOOH | -22.81 | 107.84 |
| CC(OO.)COOH | -32.37 | 101.38 |
| CC(OOH)COO. | -32.37 | 101.38 |
| C.C(OOH)COOH | -19.47 | 105.95 |
| CC.(OOH)COOH | -26.97 | 107.14 |
| CC(OOH)C.OOH | -24.57 | 104.98 |
| CCCOOH | -46.02 | 84.95 |
| $C_2COOH$ | -48.58 | 82.08 |
| HOOCCCOOH | -66.71 | 104.02 |
| CC(OOH)COOH | -68.47 | 101.16 |
| CC(=O)COOH | -71.31 | 90.93 |
| CC(OOH)C=O | -67.63 | 89.37 |
| HOOCCC=O | -65.46 | 92.21 |

Notes: Dot denotes radical site on atom to left. Carbon atoms are fully saturated with H-atoms.

Units: $\Delta H^{\circ}_{f\ 298}$, kcal / mole; $S_{298}$, cal / mol-K.

Table 2: $RO_2$ Isomerization Rate Constants ($RO_2$ => R'OOH)
($k=AT^N \exp(-E_a/RT)$, rate per H atom)

| Ring Size | Site | A [$s^{-1}$] | N | $E_a$ [kcal/mole] | $RO_2$ |
|---|---|---|---|---|---|
| 5 | prim. | 1.3E9 | 1 | 28.8 | $C_2COO.$ |
| | sec. | 5.7E8 | 1 | 26.7 | CCCOO. |
| 6 | prim. | 4.5E7 | 1 | 22.9 | CCCOO. |

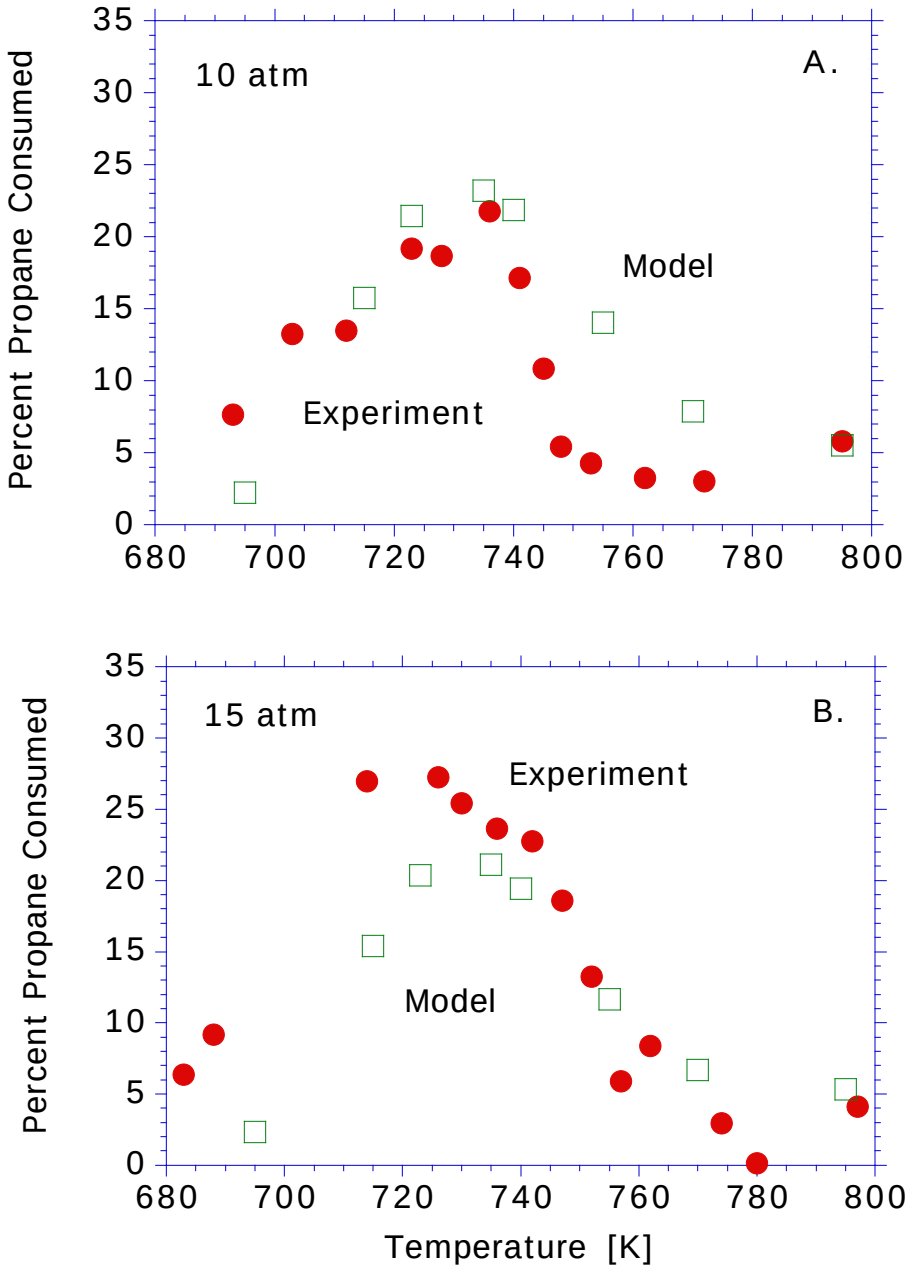
10 atm
A.
Model
Experiment
Percent Propane Consumed
0
5
10
15
20
25
30
35
680
700
720
740
760
780
800
15 atm
B.
Experiment
Model
Percent Propane Consumed
Temperature [K]

Fig. 1

10 atm Results

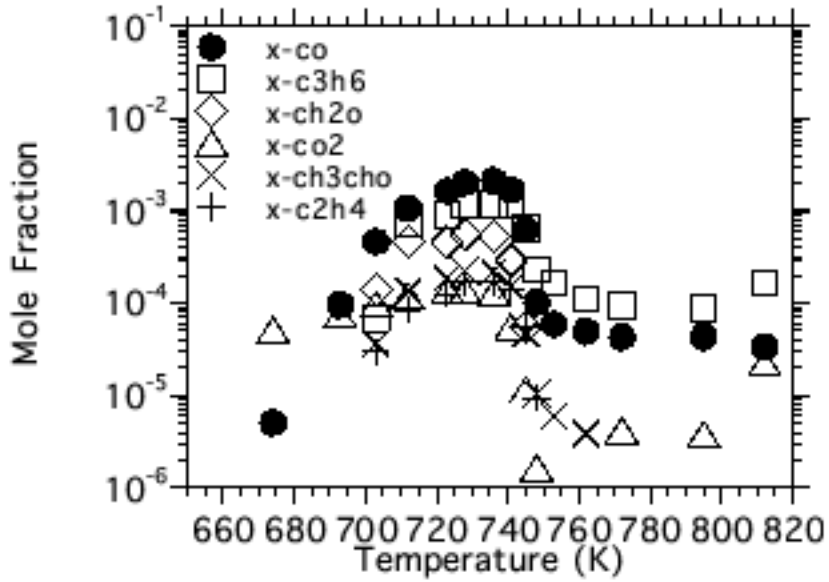


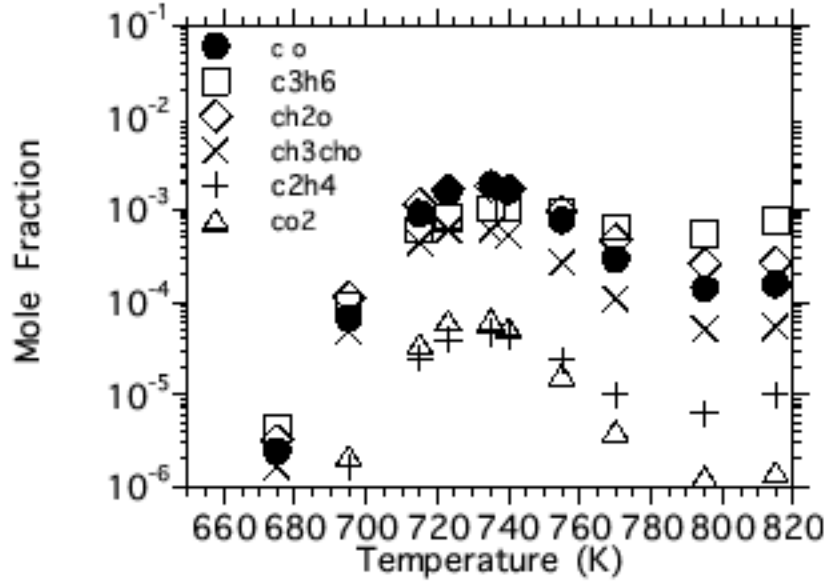


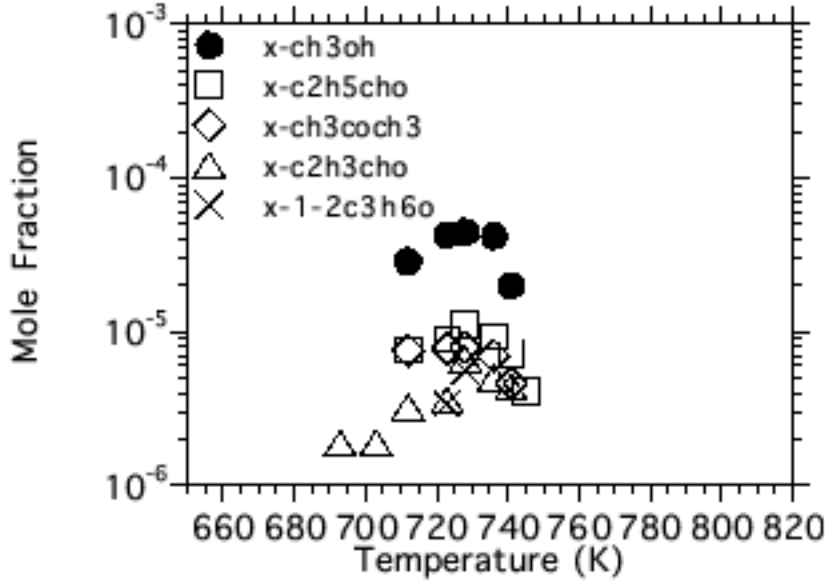


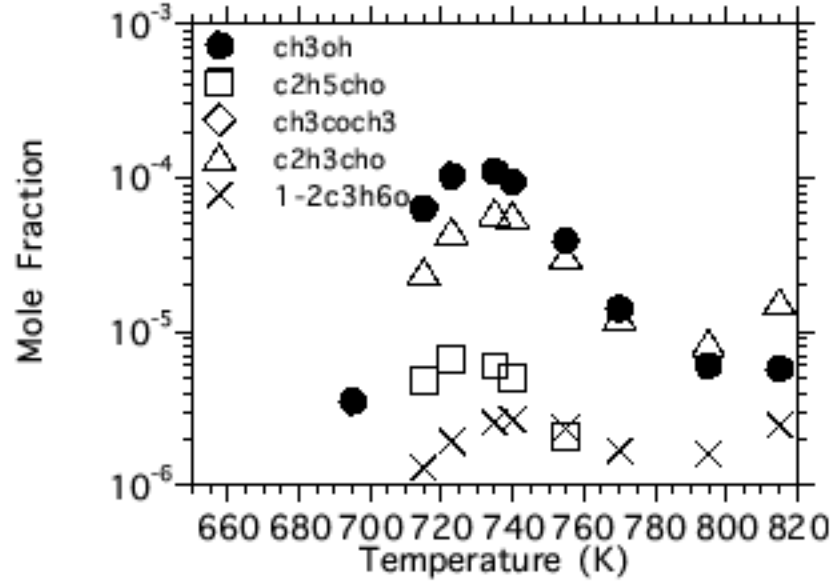

15 atm Results

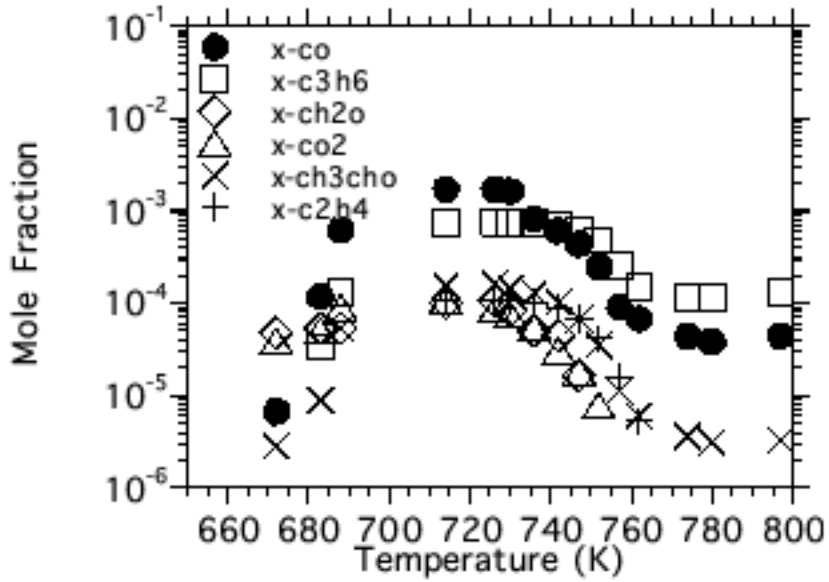


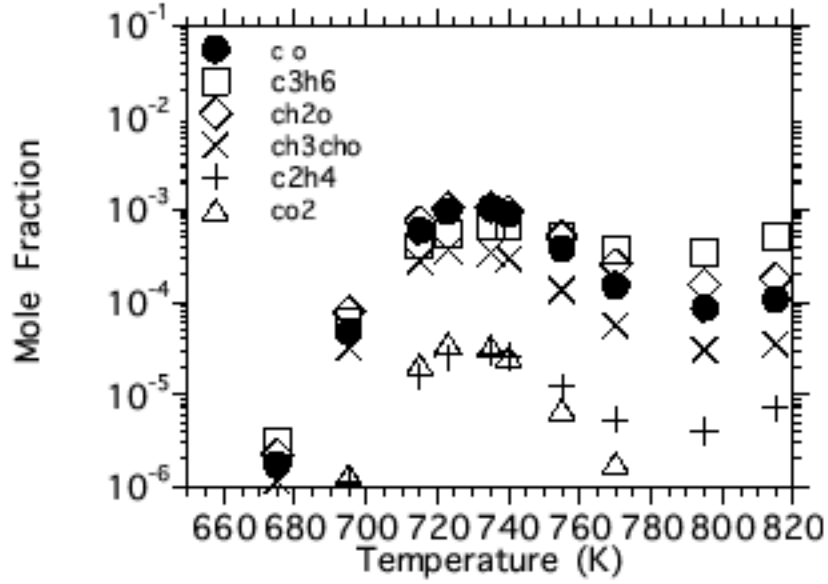


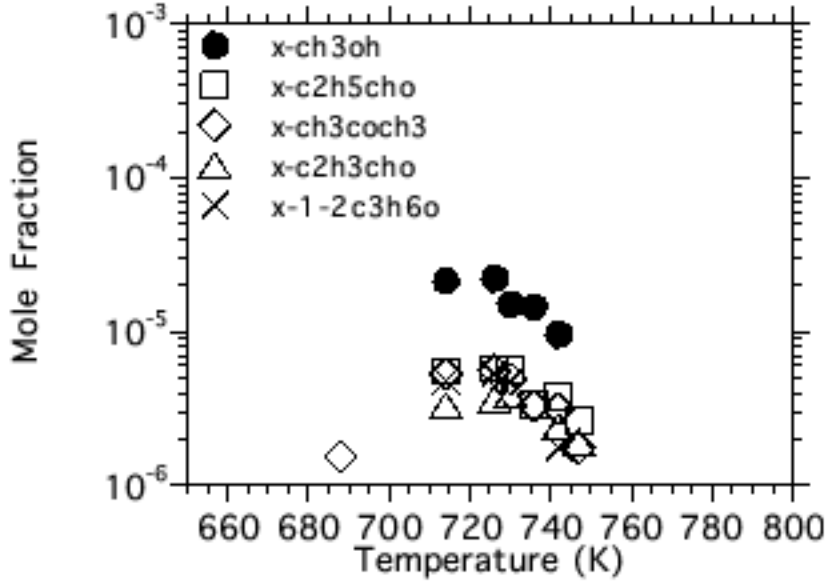


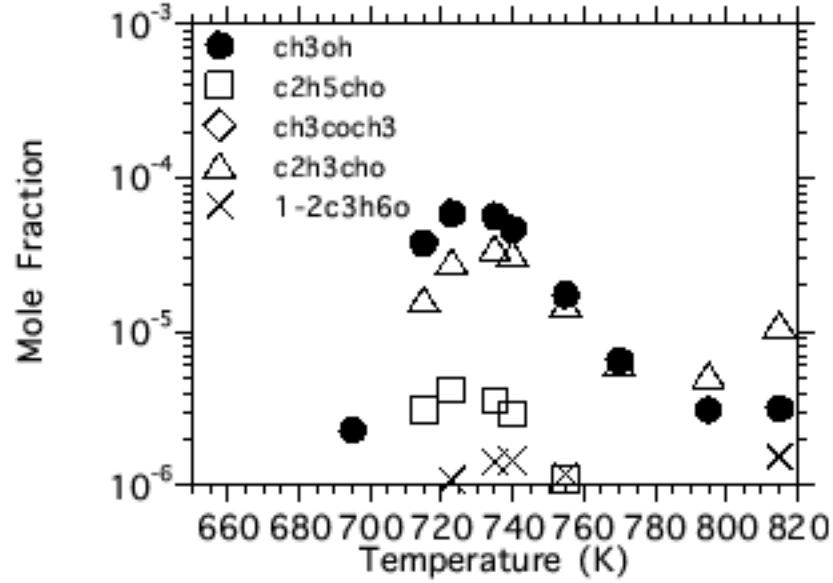

# Sensitivity at 15 atm

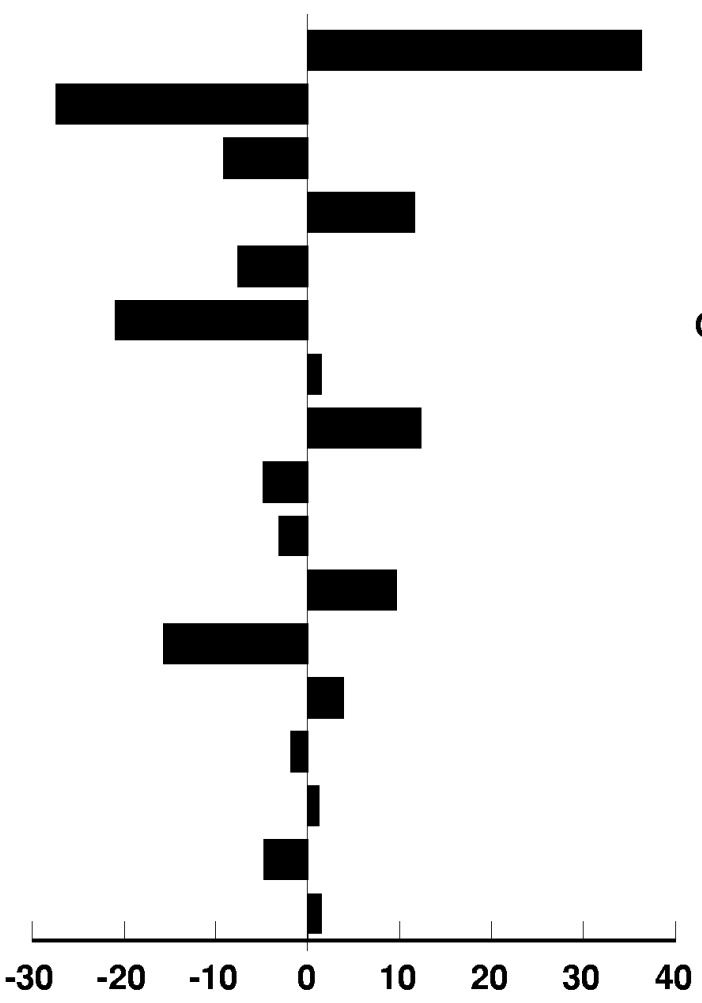


% Change in [C3H8] at 735 K

QOOH <=> R'=R'' + HO2
RH + OH <=> R + HO2
RH + HO2 <=> R + H2O2
CH2O + OH <=> HCO + H2
RO2 + XO2
OOQOOH <=> HOOR'CHO + OH
QOOH <=> RO + OH
R + O2 <=> R'=R'' + HO2
HOOR'CHO <=> A + B + OH
CH3O2H <=> CH3O + OH
H2O2 + O2 <=> HO2 + HO2
O2C3H6OOH = C3H6OOH +O2
H2O2 + OH <=> H2O + HO2
ROOH <=> RO + OH
HCO + O2 <=> CO + H
CH3O2 + RH <=> CH3O2H + R
CH3O + O2 <=> CH2O + HO2

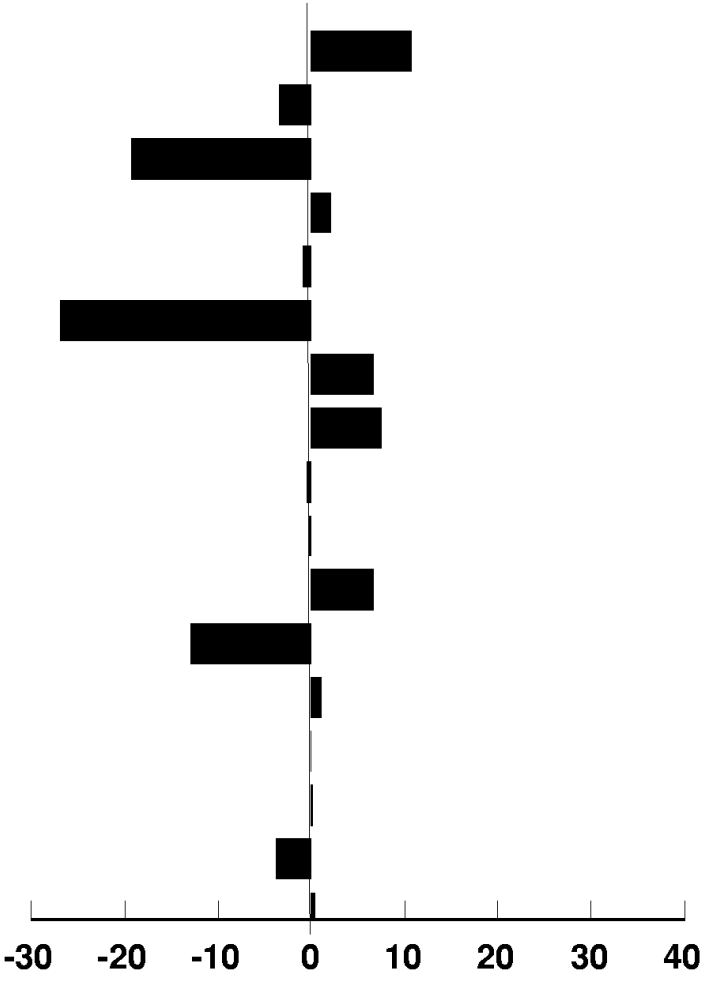


% Change in [C3H8] at 790 K